Improvement of Hydrogen Peroxide and Glucose Detection in Serum using Persistent Luminescent Nanoparticles: Impact of Synthesis Parameters and Particle Size

Zied Ferjaoui, Cyrille Richard, Jianhua Liu, Daniel Scherman, Nathalie Mignet

Improvement of Hydrogen Peroxide and Glucose Detection in Serum using Persistent Luminescent Nanoparticles: Impact of Synthesis Parameters and Particle Size

Zied Ferjaoui, Jianhua Liu, Daniel Scherman, Nathalie Mignet and Cyrille Richard *

Université Paris Cité, CNRS, INSERM, UTCBS, Unité de Technologies Chimiques et Biologiques pour la Santé, F-75006 Paris, France

Graphical Abstract:

The persistent luminescence signal of Cr-doped $ZnGa_2O_4$ (ZGO) nanoparticles is enhanced in the presence of H_2O_2 and upon excitation with UV light at 254 nm. In this work, we report that the influence of ZGO synthesis parameters, such as hydrothermal treatment at 120°C for 12 or 24 hours, calcination temperature at 500°C or 750°C, as well as nanoparticle size, ranging from 60 nm to 140 nm, strongly affect their sensitivity to H_2O_2. These distinctive factors are crucial for enhancing the effectiveness of ZGO for the *in vitro* detection of H_2O_2 and glucose.

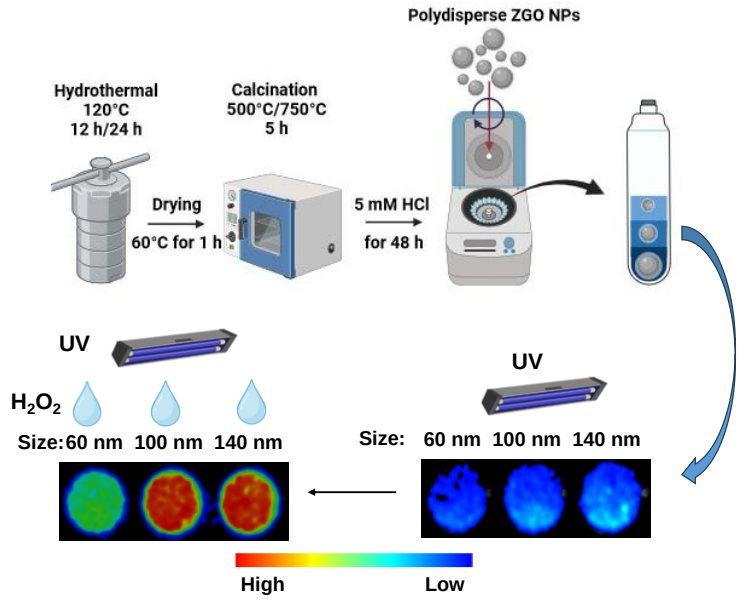

Abstract

Persistent Luminescent Nanoparticles (PLNPs) emit prolonged light after excitation, allowing getting images with high signal-to-noise ratio, making them particularly beneficial for *in vitro* biodetection. In this study, we report the preparation of a library of gallium and zinc-based Persistent Luminescent Nanoparticles doped with chromium ($ZnGa_2O_4:Cr^{3+}$) through two distinct syntheses conducted at 120°C for 12 hours or 24 hours, followed by a calcination at 500°C or 750°C. Using centrifugation, and starting from polydisperse samples, we demonstrated the ability to achieve different sizes in a monodisperse manner. Furthermore, our research revealed that $ZnGa_2O_4:Cr^{3+}$ (ZGO) nanoparticles react differently with hydrogen peroxide (H_2O_2) based on their size, synthesis duration, and calcination temperature. We observed the most significant amplification of persistent luminescence for ZGO particles prepared at 120°C for 12 hours and calcinated at 500°C, with a size of approximately 100 nm, in the presence of 100 mM H_2O_2 (later named ZGO-2). This study enabled the detection of H_2O_2 in serum without autofluorescence using the developed PLNPs, with a detection limit of up to 2.1 µM and a recovery rate of around 99%. Additionally, we designed a glucose test for based on the responsiveness of ZGO PLNPs to H_2O_2. Using glucose oxidase, the glucose detection limit in serum was established around 0.13 µM, with a detection range between 0 - 5 µM. These findings could open new avenues to further control the size, synthesis, calcination temperature, and persistent luminescence of PLNPs, thus enhancing their utility in the development of new *in vitro* biosensors**.**

Keywords: PLNPs; ZGO; H_2O_2; glucose; *in vitro*, biosensors

Introduction

Hydrogen peroxide plays a crucial role in various fields, from medicine to environmental and food industries, due to its numerous applications[1]. Used as a medical disinfectant, food bleaching agent, and oxidant in biology, H_2O_2, is although a natural by-product of cellular metabolism, that can cause severe cellular damage when in excessive cellular concentration[2]. This accumulation can lead to detrimental oxidative effects, damaging proteins, lipids, and even DNA, thereby threatening the integrity of biological systems[3].

On the other hand, glucose, an essential molecule in human physiology, represents the primary source of energy for bodily cells[4]. It is indispensable for providing necessary nutrients and fuelling metabolic activities[5]. The blood concentration of glucose serves as a crucial indicator to diagnose conditions such as hypoglycemia (low glucose levels) or diabetes (elevated glucose levels)[6][7].

Hence, the precise control and detection of H_2O_2 and glucose is vital to ensure health and safety, both in medical contexts and other application domains[8]. The development of reliable methods for detecting these compounds plays a critical role in preserving human health and well-being, as well as monitoring various biological and environmental processes[9]. Over the decades, several analytical techniques, such as fluorescence[10], electrochemistry[11], colorimetric methods[12], and chemiluminescence[13], have been exploited to detect these compounds. Among them, the chemiluminescence method is of particular interest due to its high reactivity, speed, affordability, and simplicity[14]. For this method, there is a growing emergence of nanomaterials exhibiting peroxidase-like properties[15]. For example, Shao-Bin He et al[16] have developed platinum nanoparticles coated with a bovine serum albumin structure, demonstrating enhanced peroxidase-like activities. These nanoparticles are effectively used to detect H_2O_2 through a colorimetric assay in a concentration range of 5 to 250 µM. Additionally, they have been applied to quantify glucose in human serum, exhibiting a linear response in the concentration range of 10 to 120 µM, with a detection limit of 2 µM. This demonstrates a high correlation with the standard glucose method (R^2 = 0.997 within the 95% confidence interval). Similarly, Mohammad Javad Chaichi et al[17] developed an innovative biosensor to detect glucose via the chemiluminescence of hydrogen peroxide generated by an enzymatic reaction of glucose oxidase. This method relies on the efficient covalent immobilization of glucose oxidase on Fe_3O_4-chitosan nanoparticles, facilitated by glutaraldehyde as a cross-linking agent. In the presence of gold nanoparticles, they demonstrated remarkable catalytic activity in hydrogen peroxide generation. Through

response surface methodology, the optimal conditions for glucose oxidase immobilization were determined, allowing precise glucose detection in a range from 1×10^{-4} to 8.5×10^{-7} mol L^{-1}, with a detection limit of 4.3×10^{-7} mol L^{-1} and excellent reproducibility (RSD < 3.1%). Jianxin Xie et al.[18] synthesized Co_3O_4 nanoparticles using a hydrothermal method. These particles were used to enhance the chemiluminescence (CL) of the luminol-H_2O_2 system. Results showed that 3-aminophthalate was the CL luminophore, indicating that the improvement in CL was due to the catalytic effect of Co_3O_4 nanoparticles, acting as electron transfer accelerators and radical generators. Based on this catalytic activity towards H_2O_2, a simple and selective CL test for H2O2 was developed, displaying a linear relationship between CL intensity and H_2O_2 concentration in the range of 1.0×10^{-8} to 1.0×10^{-5} mol L^{-1}, with a detection limit of 1.1×10^{-9} mol L^{-1}. Utilizing the glucose oxidase-catalyzed reaction, sensitive glucose detection was achieved within a linear range from 1.0×10^{-7} to 1.0×10^{-5} mol L^{-1} and a detection limit of 8.0×10^{-8} mol L^{-1}. This method was successfully applied to determine H_2O_2 in rainwater and glucose in serum samples.

Despite the numerous advantages of the chemiluminescence method, it still has some limitations[19], [20]. The chemiluminescence detection technique is based on an enzymatic reaction that produces light, detected by a CCD camera recording photons and generating an image based on the generated luminescence. However, this enzymatic reaction is dynamic and evolves over time, requiring careful optimization of reaction times and imaging techniques[21]. Furthermore, this method, based on light emission from nanomaterials, encounters limitations such as a high background and low stability of reagents[22]. Additionally, the nanomaterials used can be costly, further limiting their widespread adoption. Moreover, the relatively complex synthetic pathways have hindered their large-scale use [23]. Furthermore, while most chemiluminescence-based sensors exhibit impressive performances in laboratory studies, their efficiency significantly decreases when used in field applications (POC) [24]. Non-specific surface adsorption could be mitigated by developing new surface modification techniques [24].

A new detection method based on Persistent Luminescent Nanoparticles (PLNPs) is currently under development and holds great promise for *in vitro* applications [25], [26]. Thanks to this persistent luminescence, these nanoparticles can be detected and accurately tracked, even in complex environments, making them a valuable tool for biomedical research, early disease diagnosis, and monitoring of in vitro biological reactions[27], [28]. Furthermore, their colloidal stability in aqueous environments, insensitivity to visible light, and ease of synthesis make

them an efficient choice for *in vitro* or *in vivo* biodetection, providing a significant advantage over other nanomaterials [29],[25].

Our research group has focused on developing various PLNPs, notably $ZnGa_2O_4$, for *in vitro* and *in vivo* biodetection[30],[31],[32]. A previous groundbreaking study by our group revealed the unexpected impact of H_2O_2 on the persistent luminescence signal (PLS) of ZGO nanoparticles [26]. In the presence of H_2O_2, the intensity of the emission signal of ZGO was increased, thereby allowing to be applied in biosensing [26]. Indeed, a detection limit of approximately 49.4 µM H_2O_2 in PBS was determined using ZGO with a size of around 80 nm (determined by DLS), prepared at 120°C for 24 hours and calcined at 500°C. Additionally, with the same ZGO, a detection limit of around 35.8 µM glucose in PBS was achieved. This pioneering study employs, for the first time, the enhancement of persistent luminescence signal induced by the presence of H_2O_2 for biosensitivity, offering new perspectives for the precise detection of these key compounds[26].

In this study, our main objective was to improve the sensitivity of ZGO nanoparticles toward H_2O_2. We pursued several approaches to achieve this. We explored the impact of ZGO nanoparticle synthesis by varying the synthesis time between 12 and 24 hours while maintaining the temperature at 120°C. Then we investigated two distinct calcination temperatures, namely 500°C and 750°C (Figure 1). Finally, in this study, we applied a simple method to generate nanoparticles of different sizes with uniform distribution resulting from these various syntheses. Our results indicate that centrifugation allows to obtain rapidly nanoparticles of different size, ranging between 40 nm and 180 nm and of low polydispersity. We observed a more significant signal amplification for nanoparticles with a size of 100 nm, calcined at 500°C compared to those calcined at 750°C, regardless of the synthesis durations, whether it was 12 or 24 hours. Concurrently, our tests revealed a detection limit of approximately 2.1 µM for H_2O_2 and 0.13 µM for glucose using these nanoparticles in serum. These promising results suggest that these nanoparticles represent a significant advancement for *in vitro* detection of H_2O_2 and glucose.

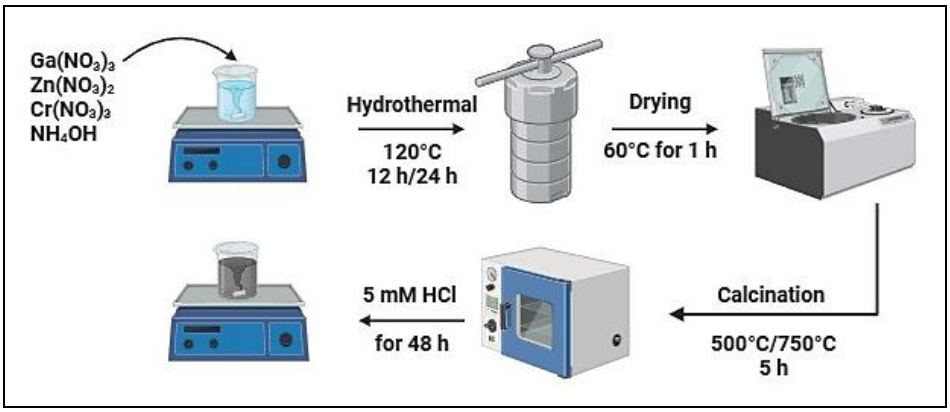

Figure 1: Schematic illustration of the hydrothermal synthesis of ZGO nanoparticles

Results and discussion

ZGO preparation and size- isolation

ZGO nanoparticles were synthesized using the hydrothermal technique in two distinct processes as described in the experimental section. Specifically, these syntheses were carried out at a temperature of 120 °C for 12 or 24 hours, followed by the calcination of the samples at either 500 °C or 750 °C. The four powders obtained under different synthesis conditions were grounded for 1 hour in the presence of HCl (5 mM), and then stirred in an HCl solution for 48 hours. For each synthesis, initial highly polydisperse samples, termed as "raw samples," were obtained. To achieve monodisperse ZGO fractions of three different sizes, we conducted three successive centrifugation steps. An overview of the protocol is shown in Figure 2. For instance, the raw sample from the synthesis carried out at 120°C during 12 hours and calcined at 500°C was transferred into 50 ml tubes, then centrifuged at 4600 rpm for 30 minutes. The supernatant was collected and labelled as "ZGO-1." Subsequently, the residue remaining in the 50 ml tube, containing most of the nanoparticles, was resuspended in a solution of 20 mL of 5 mM HCl. The resulting dispersion was centrifuged again at 4600 rpm for 10 minutes, and the collected supernatant was named "ZGO-2," while the residue was re-suspended in a 20 mL solution of 5 mM HCl and centrifuged once more at 2500 rpm for 5 minutes, and the supernatant named ZGO-3. These steps were sequentially repeated to obtain three relatively monodisperse ZGO fractions for the others raw samples prepared at 120°C for 12 hours and calcined at 750°C (ZGO-4 to 6), and likewise for samples prepared at 120°C for 24 hours and calcined at both 500°C (ZGO-7 to 9) and 750°C (ZGO-10 to 12). The samples obtained after each centrifugation were named ZGO-1, ZGO-2, and ZGO-3, and ZGO-4, ZGO-5, and ZGO-6, respectively, for samples calcined at 500 °C and 750 °C and prepared at

120 °C for 12 hours. As for the samples calcined at 500 °C and 750 °C and prepared at 120 °C for 24 hours, the fractions were named ZGO-7, ZGO-8, ZGO-9, and ZGO-10, ZGO-11, and ZGO-12, respectively. For this, we have conducted several systematic experiments to determine the optimal centrifugation speeds and durations required to obtain these well-defined and monodisperse ZGO nanoparticles. The optimal size isolation conditions are presented in Figure 2 and Table S1.

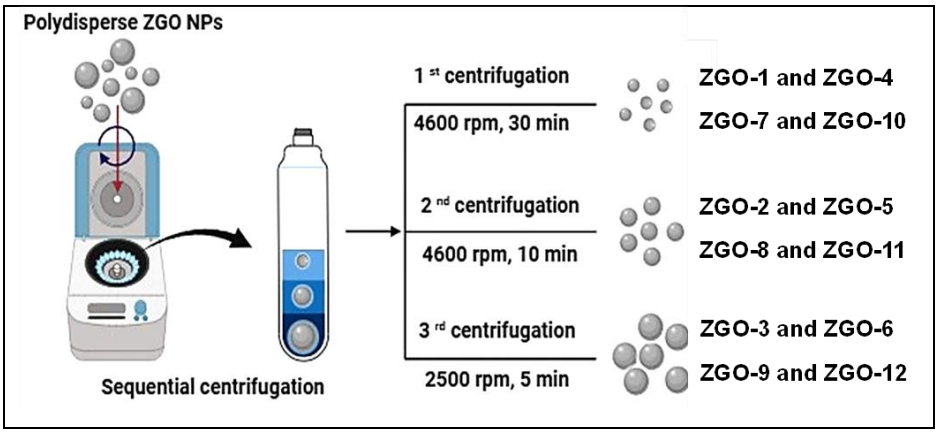

Figure 2. Schematic overview of the protocol to obtain monodisperse ZGO NPs of a particular size from a polydisperse raw mixture of ZGO NPs using sequential centrifugation.

Despite the numerous previous publications describing the synthesis of ZGO nanoparticles, the methods and technologies for their size-based separation remain relatively limited. Encarnación Arroyo et al.[33] developed $ZnGa_2O_4:Cr^{3+}$ nanoparticles using the microwave-assisted hydrothermal method. This method allows particle size adjustment from 300 nm to 30 nm by modifying the concentrations of Zn^{2+} and Cr^{3+} precursors in the initial solutions. Their study demonstrates that particles without Cr (0% Cr) and synthesized from zinc nitrate have an average diameter of 300 nm, while those obtained from zinc acetate have a diameter of 150 nm. Thus, using zinc acetate instead of zinc nitrate as a Zn source halves the particle size. This phenomenon could be attributed to the superior complexing ability of acetate over nitrate, which slows down the release of necessary Zn^{2+} cations for precipitation, affecting the particle nucleation and growth kinetics, thereby influencing the final nanoparticle size. Sridhar G et al.[34] synthesized $ZnGa_{2-x}Cr_xO_4$ nanoparticles emitting in the NIR red range. These nanoparticles were obtained through a simple co-precipitation, and the impact of

annealing was analyzed over a temperature range from 600 to 1200 °C. During this annealing step, the crystallite size evolved from 12 nm to 73 nm, and a color transition towards a pink hue appeared beyond 1000 °C, suggesting dopant diffusion. This research demonstrates the possibility of regulating nanoparticle size based on the temperature used during the co-precipitation process. The study by York E et al.[35] focused on preparing $ZnGa_2O_4:Cr^{3+}$ nanoparticles using the liquid-solid-solution solvothermal method. The nanoparticles obtained using propanol (ZGOP) and ethanol (ZGOE) had a quasi-spherical shape and a unimodal size distribution, with average diameters of 7.1 nm and 7.7 nm, respectively. Conversely, samples prepared with methanol (ZGOM) displayed a bimodal size distribution, combining small spheroidal particles (10.6 nm) and larger triangular particles (64.4 nm). To obtain larger nanoparticles, ZGOE from the first synthesis (designated ZGOE1) were used as seeds to produce larger nanoparticles. This process involved adding the ZGOE1 seed suspension to oleic acid, followed by cyclohexane evaporation under an argon atmosphere. Subsequently, a mixture containing Zn, Ga, and Cr precursors was added to the previous mixture, followed by hydrothermal treatment and a similar washing process used for ZGOE1. The resulting nanoparticles were labeled as ZGOE2. This process was repeated to obtain even larger nanoparticles, called ZGOE3, using ZGOE2 as seeds. The results showed hydrodynamic diameters measured by DLS of 19.1 nm, 26.1 nm, and 35.6 nm, respectively, for ZGOE1, ZGOE2, and ZGOE3.

Compared to the aforementioned techniques, the centrifugation method presented here is somewhat less time-consuming and labor-intensive, yet it is also easier to implement and more widely applicable, as it does not require specialized equipment nor multiple syntheses. The use of centrifugation proved to be crucial in a previous study by our team for the precise separation and selection of lanthanide-doped PLNP based on their diameter[36]. The hydrodynamic diameter variation of PLNP between 80 and 180 nm was achieved through successive centrifugation steps. For instance, isolating 180 nm PLNP from the initial polydisperse suspension required centrifugation at 4500 rpm for 5 minutes, a procedure extended to 30 minutes to obtain 120 nm PLNP. The centrifugation steps enabled the recovery of the selected PLNP in the supernatant, assessed by dynamic light scattering, before concentrating them to achieve standardized final suspensions at 5 mg mL^{-1}. This process proved instrumental in obtaining specific-sized samples, thereby contributing to an accurate assessment of nanoparticle biodistribution in our in vivo experiments[36]. The results of this study regarding the size and polydispersity of ZGO formulations, obtained through DLS, are

presented in Figure 3 and table S2. The reported DLS values, based on intensity and corresponding to the mean size, were calculated by performing at least three measurements on the same sample. The mean sizes of samples prepared at 120 °C for 12 hours are approximately 85 nm ± 0.5 nm (ZGO-1), 103 nm ± 4 nm(ZGO-2), and 128 nm ± 2 nm (ZGO-3) for samples calcined at 500 °C and approximately 85 nm ± 1.3 nm (ZGO-4), 104 nm ± 0.6 nm (ZGO-5), and 146 nm ± 1 nm (ZGO-6) for those calcined at 750 °C (Figure 2a). Regarding samples prepared at 120 °C for 24 hours, three size fractions of approximately 67 nm ± 3 nm (ZGO-7), 95 nm ± 5 nm (ZGO-8), and 139 nm ± 4 nm (ZGO-9) were obtained for samples calcined at 500 °C, and approximately 41 nm ± 3 nm (ZGO-10), 86 nm ± 4 nm (ZGO-11), and 140 nm ± 5 nm (ZGO-12) for those calcined at 750 °C. The DLS results reveal that the size gradually increases using our centrifugation protocol. The polydispersity index (PDI) values of the raw sample range from 0.2 to 0.3 (before centrifugation) for the synthesis at 120 °C for 12 hours, while the synthesis at 120 °C for 24 hours exhibits a PDI greater than 0.3. Conversely, for samples ZGO-1 to ZGO-12, all PDIs ranged between 0.1 and 0.18 (after centrifugation) (Figure 3b). In conclusion, these results suggest that our sequential centrifugation protocol is highly effective in obtaining rapidly relatively monodispersed ZGO formulations.

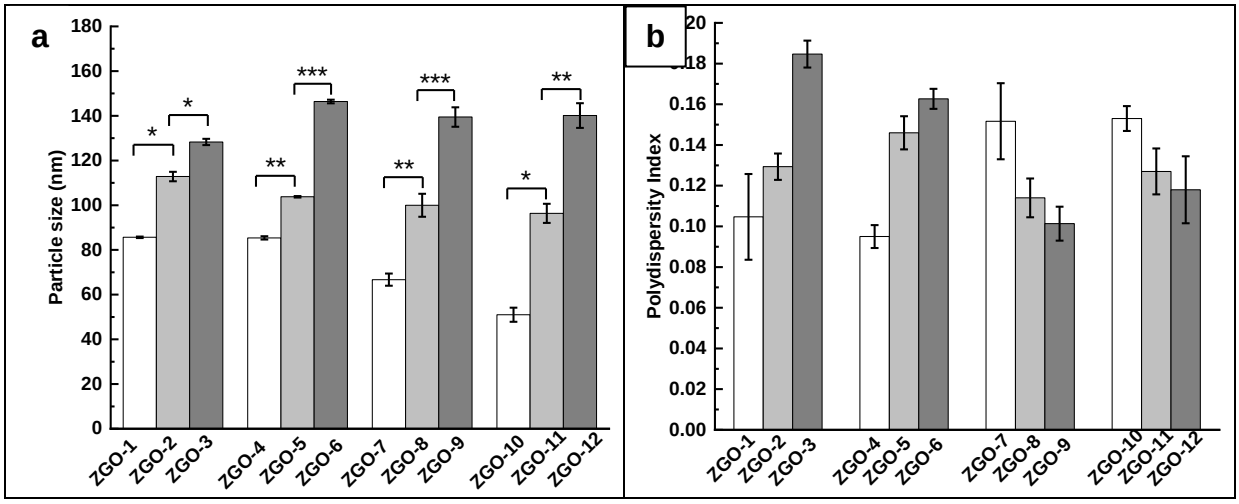

Figure 3. (a) Analysis of nanoparticle size and (b) PDI obtained using DLS. Results represent average ± standard deviation. *p< 0.05, **p< 0.01, ***p< 0.001

Evaluating ZGO PLS

In order to study and assess the sensitivity of the different samples developed in the presence of H_2O_2, our objective was to analyze their PLS under conditions both with or without H_2O_2.

We conducted a comprehensive analysis to evaluate both the impact of various synthesis and calcination conditions, as well as the variation of the size of ZGO particles, on the influence regarding this phenomenon.

To initiate our investigation, we measured the persistent signal emitted after a 254 nm UV excitation for 40 seconds across all nanoparticles dispersed in H_2O_2-free PBS. The results showed a lower luminescence intensity (in counts) production for ZGO-1 to ZGO-6 particles synthesized for 12 hours at 120°C compared to ZGO-7 to ZGO-12 prepared in 24 hours (Figure 4). Additionally, a similar trend was observed between samples calcined at 500°C and those calcined at 750°C. These observations indicate a significant impact of the synthesis duration (12 or 24 hours), calcination temperature (500°C or 750°C), as well as size on the optical properties, such as the emitted signal intensity, of ZGO particles.

A noticeable variation in signal intensity was observed in relation to particle size. Across all tested synthesis conditions, it was noted that the signal intensity increased proportionally with the particle size. For instance, for ZGO nanoparticles synthesized at 120°C for 12 hours, then calcined at 500°C (ZGO-1, ZGO-2, and ZGO-3), these sizes exhibited significant differences in count levels: 29 ± 3, 50 ± 4, and 74 ± 4, respectively, with a P-value < 0.05 (Figure 4). The size of ZGO plays a crucial role in their optical properties due to structural modifications, surface alterations, and electronic properties at the nanoscale, directly impacting the intensity of the persistent luminescent signal[37],[38]. Furthermore, the signal intensity results emitted by ZGO calcined at 750°C were almost 10 times higher than those calcined at 500°C[26]. Specifically, ZGO-4, ZGO-5, and ZGO-6 samples showed respective counts in the range of 326 ± 55, 456 ± 26, and 515 ± 33. Similarly, the synthesis duration of either 12 hours or 24 hours at 120°C also demonstrated an impact on the emitted signal by ZGO-10, ZGO-11, and ZGO-12 samples, with counts estimated at approximately 452 ± 8, 897 ± 28, and 960 ± 29, respectively. This highlights the direct impact of synthesis duration on the luminescent performances of ZGO nanoparticles, providing intriguing avenues for the optimization and control of these properties. A recent study conducted by Alexandre Gerus et al.[39] involved the preparation of $ZnGa_2O_4:Cr^{3+}$ using a hydrothermal method at 200°C, followed by calcination at different temperatures. The results revealed that varying the synthesis conditions alter the distribution of trap depths by modifying the occupancy of Zn^{2+} and Ga^{3+} sites within the spinel structure, thereby impacting the duration and intensity of persistent luminescence. Indeed, higher calcination temperatures and an increase in particle size resulted in stronger luminescence[39].

In summary, these detailed observations offer crucial insights into the determining factors affecting the luminescence signal intensity of ZGO nanoparticles, paving the way for more effective strategies to enhance and regulate their performances for specific applications in detection and biology.

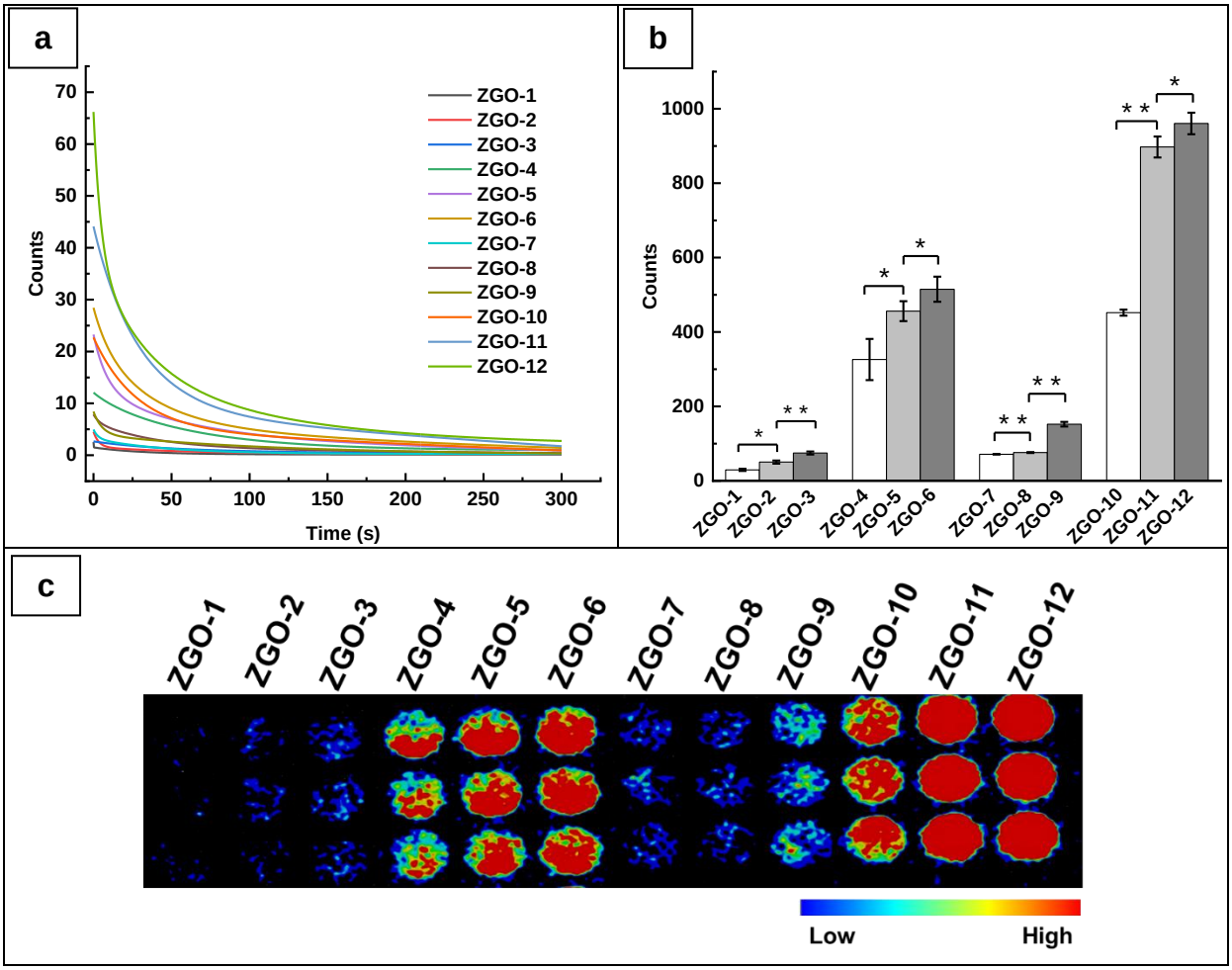

Figure 4. (a-b) Influence of synthesis conditions and particle size on PLS (experiments realized in triplicate, n = 3). (c) Image of ZGO PLS after UV excitation. Results represent average ± standard deviation. *p< 0.05, **p< 0.01

Evaluating ZGO PLS Enhancement Rates

In a previous study conducted in our laboratory, noteworthy findings were reported for ZGO nanoparticles of approximately 80 nm, synthesized at 120°C for 24 hours, demonstrating respective enhancements of 18 and for samples calcined at 500°C and 6 times for samples calcined 750°C, in the presence of 50 mM H_2O_2 [26]. To assess the combined impact of

synthesis duration, calcination temperature, and ZGO particle size on their optical properties in the presence of H_2O_2, we studied signal enhancement in response to a 100 mM H_2O_2 concentration compared to ZGO particles without H_2O_2 in PBS (Figure 5). This study revealed significant variations in enhancement ratios based on particle size from two distinct synthesis series. The smallest particles, ZGO-1 and ZGO-7, (calcined at 500°C and prepared at 120°C for 12 and 24 hours, respectively) exhibited remarkable enhancements of approximately 64 and 10 times respectively, indicating increased sensitivity to H_2O_2. Conversely, particles of similar size such as ZGO-4 and ZGO-10 (prepared at 120°C for 12 or 24 hours and calcined at 750°C) showed lower enhancements, approximately 18 and 4 times respectively, suggesting reduced effect of H_2O_2 compared to particles prepared at 120°C for 12 or 24 hours and calcined at 500°C. Moreover, medium-sized particles such as ZGO-2 and ZGO-8 (calcined at 500°C and prepared at 120°C for 12 and 24 hours, respectively) exhibited increased reactivity at a 100 mM H_2O_2 concentration, with enhancements of around 88 and 13 times respectively. In contrast, ZGO-5 and ZGO-11 (calcined at 750°C and prepared at 120°C for 12 and 24 hours respectively) displayed enhancements of approximately 20 and 6 times respectively. For particles larger than 140 nm, ZGO-3 and ZGO-6 (calcined at 500°C or 750°C and prepared at 120°C for 12 hours) showed enhancements of about 67 and 17 times respectively, while similar-sized particles ZGO-9 and ZGO-12 (calcined at 500°C or 750°C and prepared at 120°C for 24 hours) exhibited enhancements of approximately 9 and 3 times respectively. These observations reveal complex variability in ZGO response to H_2O_2, even among particles of similar size, emphasizing the importance of considering other parameters to evaluate their reactivity. Synthesis duration also emerged as a crucial factor, with increased sensitivity of ZGO synthesized for 12 hours compared to those synthesized for 24 hours at 120°C. Lastly, the results highlighted differences in reactivity based on calcination temperature, where ZGO calcined at 500°C exhibited higher enhancement ratios compared to those calcined at around 750°C. These observations underscore the complexity of ZGO responses to H_2O_2 under different experimental conditions, emphasizing the need for a comprehensive understanding to optimize ZGO-based sensors for specific detection applications.

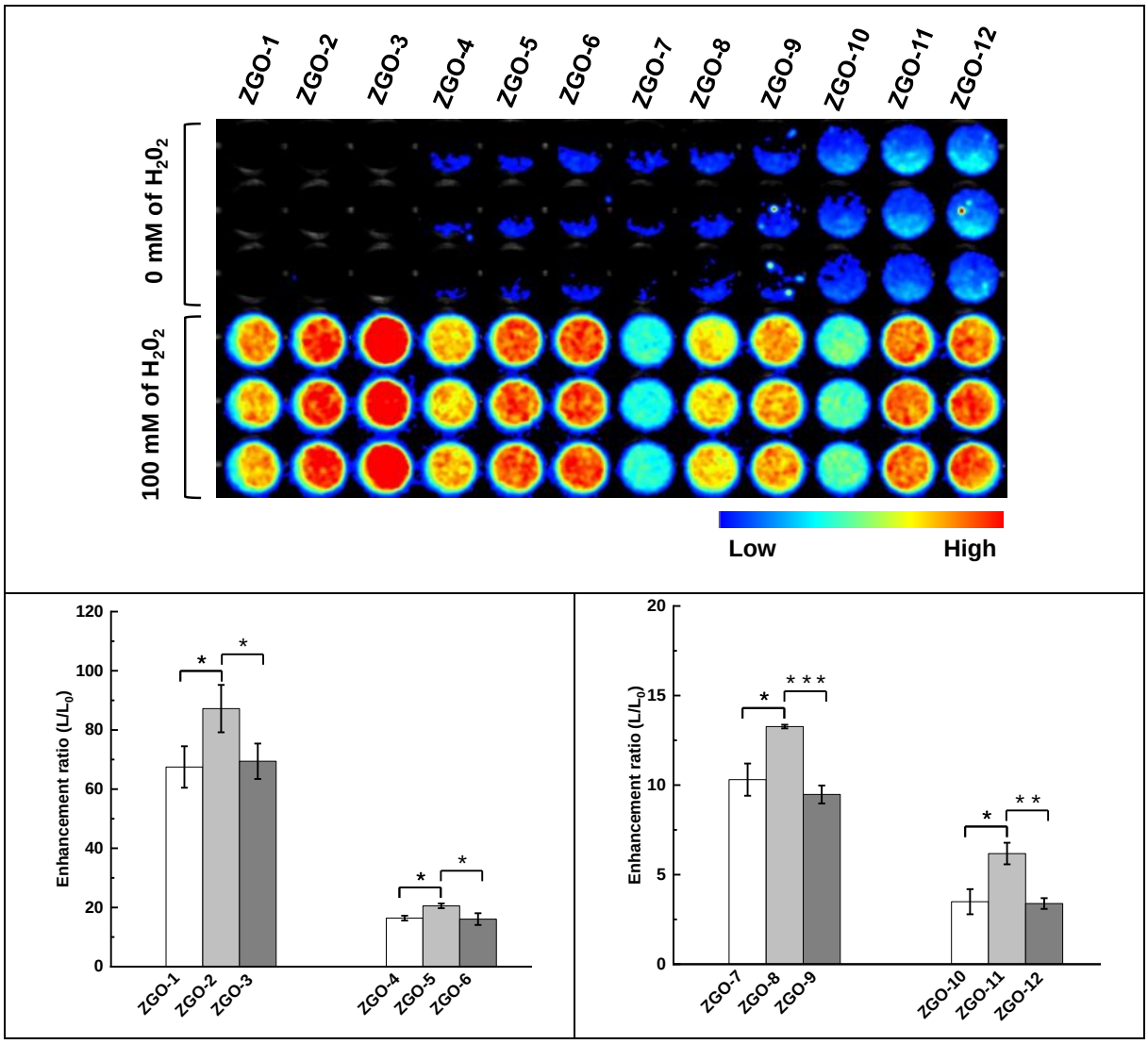

Figure 5. Impact of size on the PLS of ZGO in the absence and presence of H_2O_2. Results represent average ± standard deviation. *p< 0.05, **p< 0.01, ***p< 0.001

Overall, the size and preparation methods of ZGO nanoparticles are key parameters modulating their physicochemical properties and influencing their reactivity towards hydrogen peroxide, resulting in notable differences in their ability to amplify the signal in the presence of H_2O_2, as observed in the experiments conducted.

H_2O_2 and Glucose Detection in serum

In this section, we conducted a comprehensive analysis of H_2O_2 and glucose detection under optimal conditions using mouse serum (MS) and human serum (HS).

For this study, we selected four types of ZGO (ZGO-2, ZGO-5, ZGO-8, and ZGO-11), each exhibiting the highest signal amplification within their group in the presence of 100 mM H_2O_2. These observations were made for each synthesis condition, whether at 120°C for 12 hours or 24 hours, as well as for different calcination temperatures, either 500°C or 750°C.

Figures 6 and S2 demonstrate a linear relationship between the enhancement ratio values and H_2O_2 concentration over a broad range, from 0.05 to 1 mM for various nanoparticles in MS (Figure S2) and HS (Figure 6). These results are supported by remarkably high correlation coefficients, namely 0.999 (ZGO-2), 0.992 (ZGO-5), 0.999 (ZGO-8), and 0.990 (ZGO-11) in MS, and approximately 0.999 (ZGO-2), 0.998 (ZGO-5), 0.999 (ZGO-8), and 0.997 (ZGO-11) in HS. Moreover, the limits of detection (LOD) for ZGO-2, ZGO-5, ZGO-8, and ZGO-11 for H_2O_2 were determined to be 3.3 µM (LOQ = 10.9 µM), 77.4 µM (LOQ = 257.8 µM), 22.5 µM (LOQ = 75.1 µM), and 81.1 µM (LOQ = 270.1 µM), respectively, in MS, and approximately 2.1 µM (LOQ = 6.9 µM), 35 µM (LOQ = 115.4 µM), 8 µM (LOQ = 26.6 µM), and 39.3 µM (LOQ = 129.8 µM), respectively, in HS (Table S3). The recovery rates of H_2O_2 in spiked serum samples range from 88 to 100% (Table S3), demonstrating the precision of ZGO in H_2O_2 detection in serum.

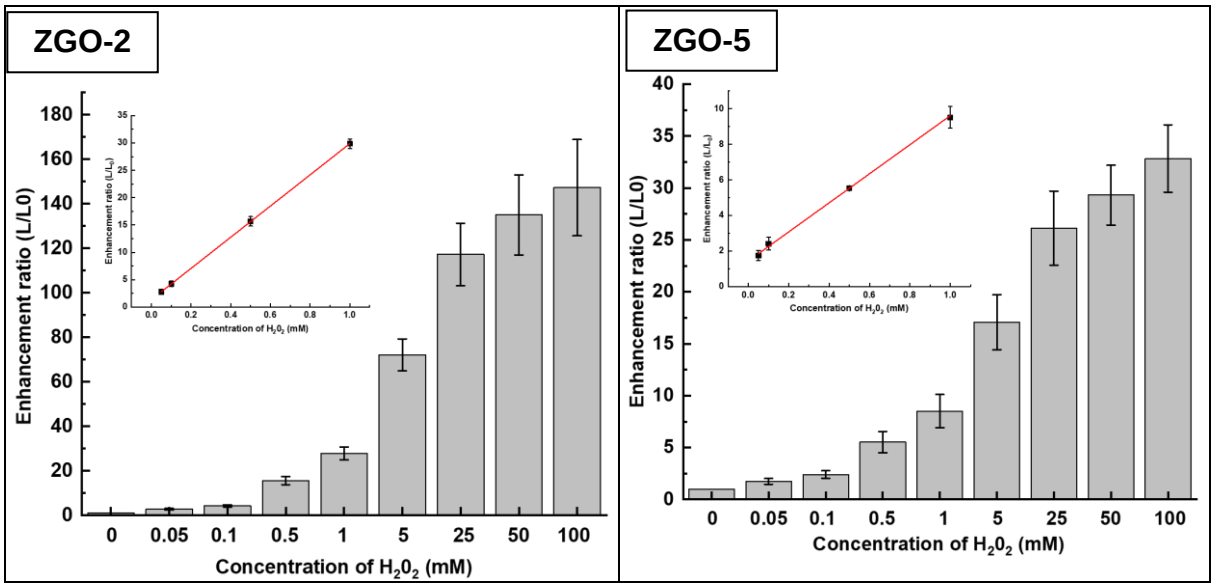

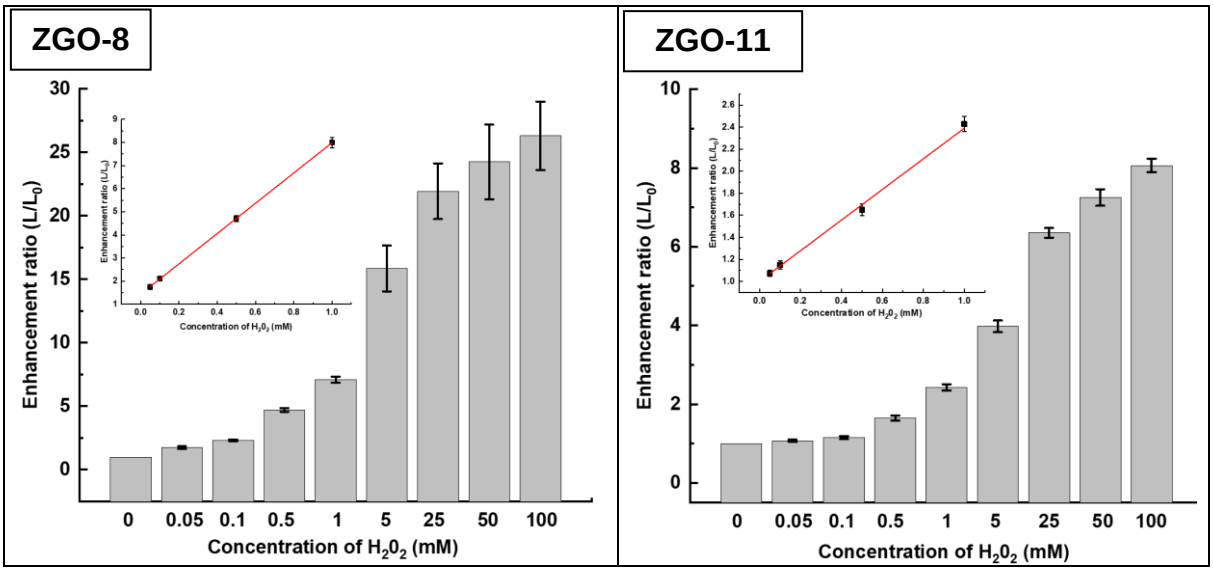

Figure 6. Enhancement ratio applied to the dosage of H_2O_2 in SH. In the inset, linear relationship between the enhancement ratio and the concentration of H_2O_2.

Our results regarding the detection of H_2O_2 in serum using ZGO reveal LOD and wider detection ranges, sometimes comparable to those reported in other studies (Table S3). Indeed, their capability of persistent luminescence allows them to emit light even after the external light source is turned off. This characteristic provides precise and prolonged detection of biological targets such as H_2O_2, even in conditions of low concentration and in environments with autofluorescence. Moreover, the direct sensitivity of these nanoparticles to specific substances such as H_2O_2 makes them highly attractive for biomedical detection applications in laboratory settings.

In the context of this study, two samples, ZGO-2 and ZGO-8, were identified as exhibiting the lowest detection thresholds for H_2O_2 in both MS and HS. These samples were particularly selected for their potential application in glucose detection. Notably, glucose oxidase (GOx), an enzyme catalyzing glucose oxidation, produces H_2O_2 as a byproduct [40]. Considering both the H_2O_2 generated from this reaction and the sensitivity of ZGO nanoparticles to H_2O_2, we conducted investigations on glucose detection using these two serum types and with ZGO-2 and ZGO-8.

Figure 7 illustrate, that the signal amplification of ZGO-2 and ZGO-8 progressively increases with rising glucose concentration. The correlation between signal amplification and glucose concentration is linear in the range of 0 to 5 µM in MS and approximately 0.995, 0.993, 0.990, and 0.991 in HS. The LODs in MS for glucose is 0.07 µM (LOQ = 0.2 µM) and 0.26

µM (LOQ = 0.86 µM) for ZGO-2 and ZGO-8, respectively, while in HS, values are around 0.13 µM (LOQ = 0.4 µM) and 0.25 µM (LOQ = 0.8 µM). The recovery rates of glucose in spiked serum samples range from 95 to 99% (Table 1), highlighting the accuracy of ZGO in glucose detection in serum without autofluorescence.

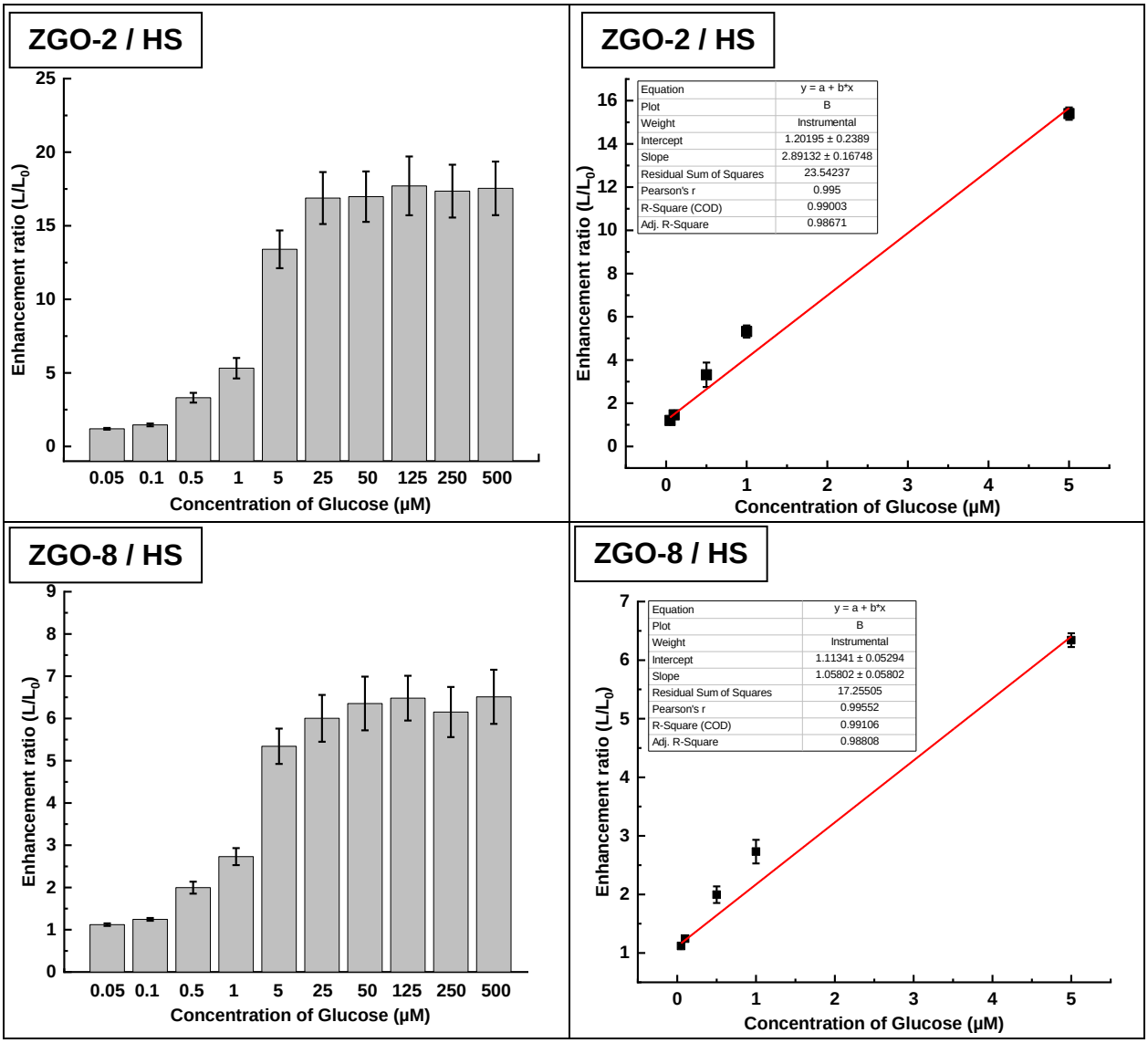

Figure 7. Enhancement ratio applied to the dosage of glucose in HS. In the inset, linear relationship between the enhancement ratio and the concentration of glucose.

To gain a better understanding of the significance of these ZGO nanoparticles in glucose biosensing, Table 1 presents results highlighting that ZGO nanoparticles have a wider linear range and lower LOD values in serum when compared to other nanomaterials (Table 1).

Table 1. Comparison of different nanoparticles for the detection of glucose

Sample	Medium	Added (mM)	Total found (mM)	Recovery (%, n=3)	Linear Range (µM)	Limit of Detection (µM)	Ref
ZGO-2	MS	0.05	0.048	96.000	0 – 5	0.07	This work
		0.1	0.098	98.000			
		0.5	0.484	96.800			
		1	0.972	97.200			
		5	4.906	98.120			
ZGO-2	HS	0.05	0 .049	98.000	0 - 5	0.13	This work
		0.1	0.095	95.000			
		0.5	0.481	96.200			
		1	0.974	97.428			
		5	4.964	99.280			
ZGO-8	MS	0.05	0.047	94.000	0 – 5	0.27	This work
		0.1	0.096	96.785			
		0.5	0.480	96.000			
		1	0.990	99.000			
		5	4.952	99.047			
ZGO-8	HS	0.05	0.049	98.000	0 – 5	0.25	This work
		0.1	0.098	98.039			
		0.5	0.497	99.426			
		1	0.977	97.744			
		5	4.945	98.913			
(GOD)-graphene-chitosan nanocomposite	PBS	…			80 – 12000	20	[41]
AgNP/F-SiO_2/GO	PBS	…			2000 -12000	310	[42]
PPDox/UCNPs	SH	2	6.11	99.5	5 – 80	0.83	[43]
SiNPs/OPD	PBS	1.00	10.49	100.29	20-1250	6.8	[44]
CuxSy	Spiked blood samples	0.5	− 0.2	40	200 - 16 000	200	[45]
		1	1.1	110			
		2	2.1	105			
		3	2.9	96.66			
		4	4	100			
Fe3O4NPs/PdNPs /g-C3N4	Serum	10	18	98	0 – 200	15	[46]
GOx/AuNPs/TA-APTES/aCC	PBS	…			0.01 – 18	3.3	[47]
Au-SiO2NP/GOx/GCE	PBS	…			0.2 – 7	0.2	[48]
Cu-Pt NPs/GCE	0.1 M of NaOH solution	…			10–750	1.8	[49]

Np-PtCu	**Near-neutral pH solutions**	**…**	**10–2000**	**0.1**	[50]
rGO/Cu–Cu2O SPCE	**Water**	**…**	**10 – 7000**	**0.06**	[51]
CuO-IL/rGO SPCE	**Diluted in PBS, pH 7.4**	**…**	**30 – 7000**	**0.19**	[52]

Conclusions

In this study, we successfully produced ZGO nanoparticles of various sizes through sequential centrifugation, based on different synthesis conditions, specifically at 120°C for 12 or 24 hours, followed by calcination at 500°C or 750°C. Furthermore, our investigations highlighted the significant influence of synthesis duration, calcination temperature, and ZGO size on enhancing the persistent luminescence of PLNPs in the presence of H_2O_2. Remarkably, the use of ZGO-2 or ZGO-8 of similar sizes (100 nm) significantly improved glucose detection, reaching approximately 0.13 µM, in HS types. Our forthcoming studies aim to delve deeper into the effect of H_2O_2 on signal amplification in ZGOs and to analyze how the size of these particles influences this amplification. These advancements promise exciting prospects for controlled synthesis of PLNPs, paving the way for their application in biosensing and *in vitro* biological detection.

Experimental section

Materials

Zinc nitrate hexahydrate (>99%), gallium oxide (99.999%), and chromium (III) nitrate nonahydrate (99.9%) were purchased from Alfa Aesar, Karlsruhe, Germany. The ammonia solution (30 wt %) and hydrochloric acid were obtained from Carlo Erba. Nitric acid (70 wt %), Phosphate Buffered Saline (PBS), Hydrogen Peroxide (30 wt %), Human Serum, Mouse Serum, Glucose Oxidase and Glucose (>99.5%) were purchased from Sigma-Aldrich. All chemicals were used as received without the need for further purification.

Preparation of ZGO Nanoparticles

The ZGO nanoparticles were synthesized according to a well-defined protocol. To begin, 1.675 g of gallium oxide (Ga_2O_3) (8,94 mmol) was put into a Teflon-coated stainless-steel autoclave and 10 mL of 35 % nitric acid (HNO_3). was added and the whole was heated to 150°C for a duration of four days.

Following this, a solution containing 0.016 g of $Cr(NO_3)_3 \cdot 9H_2O$ (0,04 mmol) and 2.668 g of $Zn(NO_3)_2 \cdot 6H_2O$ (8,97 mmol) dissolved in 10 mL of demineralized water was prepared and mixed with the previously obtained $Ga(NO_3)_3$ solution (transferred to a 100 mL round-bottom flask). Under continuous agitation, the pH of the mixture was adjusted to 7.5 by adding a 30% solution ammonia (≈ 8 mL) drop by drop. Subsequently, the resulting solution was stirred for 3 hours at room temperature and then transferred to a Teflon-coated stainless-steel autoclave. Heating was carried out at two different temperatures, either at 120 °C for 12 or 24 hours.

Once the heating process was completed, the resulting product was thoroughly washed with water and ethanol using centrifugation at 4600 rpm for 15 minutes, then dried at 60 °C for 1 hour. The resulting white powder was divided into two portions and subjected to a sintering process at respective temperatures of 500 °C and 750 °C, each for 5 hours.

To obtain ZGO particles of nanometric size, 500 mg of powder were ground for 1 hour using a mechanical grinder in the presence of 500 µL of a 5 mM hydrochloric acid (HCl) solution. Subsequently, it was transferred to 50 mL of HCl, and the suspension was stirred overnight to recover ZGO nanoparticles of various sizes. Various centrifugation steps were carried out with different speeds and durations for this purpose. Comprehensive details regarding these centrifugations are discussed in the results and discussion section of this study.

Effect of H_2O_2 on the PLS of ZGO

The effect of varying concentrations of H_2O_2 was assessed using ZGO nanoparticles synthesized through distinct conditions outlined below. Firstly, the ZGO nanoparticles were washed with distilled water and subsequently centrifuged at 14 000 g for 20 minutes to recover these ZGO nanoparticles.

Subsequently, a ZGO suspension at a concentration of 0.1 mg mL^{-1} in PBS was prepared and 50 µL were added in triplicate to a 96-well plate. Then, solutions of H_2O_2 at concentrations of 0 mM and 100 mM were prepared in PBS and 50 µL were added to the wells already containing ZGO suspensions. The resulting mixture, reaching a final volume of 100 µL, was incubated for 5 minutes at room temperature.

Persistent luminescence spectra were collected using a photon counting device (Biospace camera) after UV excitation at 254 nm for one minute. Subsequently, these spectra were analyzed using the M3 Vision software to assess the response of the ZGO nanoparticles to different concentrations of H_2O_2. This methodology allows for an appreciation of the sensitivity of ZGO nanoparticles to varying levels of H_2O_2, which is essential for characterizing their performance in the detection of this compound.

Detection of H_2O_2 in serum samples

To investigate the effects of serum on the optical properties and H_2O_2 detection, we conducted a detection study in a medium consisting of mouse serum or serum human. In brief, 50 µL of serum and solutions of H_2O_2 at different concentrations (0.05, 0.1 0.5, 5, 25, 50 and 150 mM) were added to the ZGO suspension at different concentrations (0.05 and 0.10 mg. mL^{-1}) in a 96-well plate. Subsequently, the samples, reaching a final volume of 100 µL per well, were incubated for 5 minutes. At the end of this incubation period, UV excitation at 254 nm was carried out for 1 minute. Persistent luminescence spectra were collected using a photon counting device. These spectra were then analyzed with the M3 Vision software to assess the response of ZGO nanoparticles to different concentrations of H_2O_2 in a mouse serum and human serum.

Glucose detection in serum samples

Glucose detection was carried out as follows: In a microplate, 25 µL of glucose oxidase (GOD) and 25 µL of glucose at various concentrations (0.05, 0.1, 5, 10, 20, 50, 125, 250, 500 µM), prepared in mouse serum or serum human were incubated at 37°C for 1 hour to generate H_2O_2. Subsequently, 50 µL of the ZGO suspension at different concentrations of 0.05 and 0.1 mg mL^{-1} was added. After a 1 hour of incubation of this mixture at 37°C, the increase in signal was measured and analyzed as previously described.

Method validation

The proposed method has undergone validation in accordance with the standards established by internationally recognized publications [53],[54]. This validation encompassed several key aspects such as linearity, detection and quantification limits (LOD and LOQ), selectivity, and precision.

To assess the method's linearity, graphs were constructed by studying enhancement ratios based on concentrations of H_2O_2 or glucose, ranging from 0.05 mM to 150 mM and 0.05 µM to 500 µM respectively.

Regarding sensitivity, it was determined using the Limit of Detection (LOD) (3 SD/S) and the Limit of Quantification (LOQ) (10 SD/S), utilizing the standard deviation of different blank samples (SD) and the slope of the calibration curve (S).

The method's selectivity was evaluated by observing the concentration of added H_2O_2 or glucose in relation to the measured concentrations, verifying the method's specificity (Recovery rate (%) = (Quantity measured / Quantity added) x 100).

As for precision, two aspects were studied: repeatability, assessed by conducting three analyses on five different concentrations for each analyte, and intermediate precision, evaluated over a period of three consecutive days.

Statistical Analysis

The analysis involved presenting values as the mean and standard deviation derived from a minimum of three experiments. To assess the significance between experimental groups, an unpaired Student's t-test (unless otherwise specified) was conducted, with a p-value < 0.05 considered statistically significant.

References

[1] J. E. Giaretta, H. Duan, F. Oveissi, S. Farajikhah, F. Dehghani, S. Naficy, *ACS Appl. Mater. Interfaces* **2022**, *14*, 20491.
[2] E. Feliziani, A. Lichter, J. L. Smilanick, A. Ippolito, *Postharvest Biology and Technology* **2016**, *122*, 53.
[3] K. J. A. Davies, *IUBMB Life* **2000**, *50*, 279.
[4] S.-C. Lin, D. G. Hardie, *Cell Metabolism* **2018**, *27*, 299.
[5] F. M. Matschinsky, *Diabetes* **1996**, *45*, 223.
[6] J. Kesavadev, A. Misra, B. Saboo, S. R. Aravind, A. Hussain, L. Czupryniak, I. Raz, *Diabetes & Metabolic Syndrome: Clinical Research & Reviews* **2021**, *15*, 221.
[7] J. E. Bowe, Z. J. Franklin, A. C. Hauge-Evans, A. J. King, S. J. Persaud, P. M. Jones, *Journal of Endocrinology* **2014**, *222*, G13.
[8] X. Chen, G. Wu, Z. Cai, M. Oyama, X. Chen, *Microchim Acta* **2014**, *181*, 689.
[9] Y. Qi, Y. Sun, D. Song, Y. Wang, F. Xiu, *Talanta* **2023**, *253*, 124039.
[10] J. Yuan, Y. Cen, X.-J. Kong, S. Wu, C.-L. Liu, R.-Q. Yu, X. Chu, *ACS Appl. Mater. Interfaces* **2015**, *7*, 10548.
[11] T. Liu, Y. Guo, Z. Zhang, Z. Miao, X. Zhang, Z. Su, *Sensors and Actuators B: Chemical* **2019**, *286*, 370.
[12] S. Chen, X. Hai, X.-W. Chen, J.-H. Wang, *Anal. Chem.* **2014**, *86*, 6689.
[13] S. A. Kitte, W. Gao, Y. T. Zholudov, L. Qi, A. Nsabimana, Z. Liu, G. Xu, *Anal. Chem.* **2017**, *89*, 9864.
[14] M. Haddad Irani-nezhad, J. Hassanzadeh, A. Khataee, Y. Orooji, *Molecules* **2019**, *24*, 689.
[15] Y. Jia, S. Sun, X. Cui, X. Wang, L. Yang, *Talanta* **2019**, *205*, 120139.
[16] S.-B. He, R.-T. Chen, Y.-Y. Wu, G.-W. Wu, H.-P. Peng, A.-L. Liu, H.-H. Deng, X.-H. Xia, W. Chen, *Microchim Acta* **2019**, *186*, 778.
[17] M. J. Chaichi, M. Ehsani, *Sensors and Actuators B: Chemical* **2016**, *223*, 713.
[18] J. Xie, Y. Huang, *Anal. Methods* **2011**, *3*, 1149.
[19] S. Deepa, R. Venkatesan, S. Jayalakshmi, M. Priya, S.-C. Kim, *Journal of Environmental Chemical Engineering* **2023**, *11*, 109853.
[20] M. V. Zvereva, A. V. Zhmurova, *Biophys Rev* **2023**, *15*, 963.
[21] S. T. Mathews, E. P. Plaisance, T. Kim, *Methods Mol Biol* **2009**, *536*, 499.
[22] M. M. Calabretta, M. Zangheri, D. Calabria, A. Lopreside, L. Montali, E. Marchegiani, I. Trozzi, M. Guardigli, M. Mirasoli, E. Michelini, *Sensors* **2021**, *21*, 4309.
[23] M. Yang, J. Huang, J. Fan, J. Du, K. Pu, X. Peng, *Chem. Soc. Rev.* **2020**, *49*, 6800.
[24] X. Zhang, C. Li, W. Chen, G. Wang, H. Zou, H. Liu, *Front. Chem.* **2023**, *10*, 1106791.
[25] S. Yang, W. Dai, M. Tang, J. Wang, *ACS Appl. Mater. Interfaces* **2023**, *15*, 38644.
[26] J. Liu, B. Viana, N. Mignet, D. Scherman, Y. Liu, C. Richard, *Small* **2023**, 2303509.
[27] R. M. Calderón-Olvera, E. Arroyo, A. M. Jankelow, R. Bashir, E. Valera, M. Ocaña, A. I. Becerro, *ACS Appl. Mater. Interfaces* **2023**, *15*, 20613.
[28] E. Teston, T. Maldiney, I. Marangon, J. Volatron, Y. Lalatonne, L. Motte, C. Boisson-Vidal, G. Autret, O. Clément, D. Scherman, F. Gazeau, C. Richard, *Small* **2018**, *14*, 1800020.
[29] J. Liu, T. Lécuyer, J. Seguin, N. Mignet, D. Scherman, B. Viana, C. Richard, *Advanced Drug Delivery Reviews* **2019**, *138*, 193.

[30] C. Rosticher, B. Viana, T. Maldiney, C. Richard, C. Chanéac, *Journal of Luminescence* **2016**, *170*, 460.
[31] T. Lécuyer, M.-A. Durand, J. Volatron, M. Desmau, R. Lai-Kuen, Y. Corvis, J. Seguin, G. Wang, D. Alloyeau, D. Scherman, N. Mignet, F. Gazeau, C. Richard, *Nanoscale* **2020**, *12*, 1967.
[32] T. Lécuyer, N. Bia, P. Burckel, C. Loubat, A. Graillot, J. Seguin, Y. Corvis, J. Liu, L. Valéro, D. Scherman, N. Mignet, C. Richard, *Nanoscale* **2022**, *14*, 1386.
[33] E. Arroyo, B. Medrán, V. Castaing, G. Lozano, M. Ocaña, A. I. Becerro, *J. Mater. Chem. C* **2021**, *9*, 4474.
[34] S. G., D. Hebbar N., S. G. Menon, P. M. Lewis, K. S. Choudhari, R. E. Kroon, H. C. Swart, S. D. Kulkarni, *Optical Materials* **2022**, *123*, 111919.
[35] Y. E. Serge-Correales, D. Neumeyer, S. Ullah, R. Mauricot, Q. Zou, S. J. L. Ribeiro, M. Verelst, *Langmuir* **2023**, *39*, 1495.
[36] T. Maldiney, A. Lecointre, B. Viana, A. Bessière, M. Bessodes, D. Gourier, C. Richard, D. Scherman, *J. Am. Chem. Soc.* **2011**, *133*, 11810.
[37] Y. Sheng, L.-D. Liao, A. Bandla, Y.-H. Liu, N. Thakor, M. C. Tan, *ACS Biomater. Sci. Eng.* **2016**, *2*, 809.
[38] S. E. Crawford, M. J. Hartmann, J. E. Millstone, *Acc. Chem. Res.* **2019**, *52*, 695.
[39] A. Gerus, V. Boiko, V. C. Ciaramitaro, M. L. Saladino, D. Hreniak, *Materials Research Bulletin* **2023**, *168*, 112473.
[40] L.-H. Fu, C. Qi, J. Lin, P. Huang, *Chem. Soc. Rev.* **2018**, *47*, 6454.
[41] X. Kang, J. Wang, H. Wu, I. A. Aksay, J. Liu, Y. Lin, *Biosensors and Bioelectronics* **2009**, *25*, 901.
[42] W. Lu, Y. Luo, G. Chang, X. Sun, *Biosensors and Bioelectronics* **2011**, *26*, 4791.
[43] T. Zhao, Y. Li, X. Zhang, H. Lyu, Z. Xie, *Microchemical Journal* **2023**, *186*, 108363.
[44] C. Yang, N. Gao, Y. Liu, H. Zhao, J. Jing, X. Zhang, *New J. Chem.* **2021**, *45*, 19515.
[45] P. Tetyana, N. Mphuthi, A. N. Jijana, N. Moloto, P. M. Shumbula, A. Skepu, L. S. Vilakazi, L. Sikhwivhilu, *Nanomaterials* **2023**, *13*, 481.
[46] X. Zhang, C. Sun, R. Li, X. Jin, Y. Wu, F. Fu, *Anal. Chem.* **2023**, *95*, 5024.
[47] Y. Zhu, Y. Qi, M. Xu, J. Luo, *Colloids and Surfaces A: Physicochemical and Engineering Aspects* **2023**, *661*, 130908.
[48] S. Kumar-Krishnan, M. Guadalupe-Ferreira García, E. Prokhorov, M. Estevez-González, R. Pérez, R. Esparza, M. Meyyappan, *J. Mater. Chem. B* **2017**, *5*, 7072.
[49] C. Wang, X. Yang, G. Zhu, T. Wang, D. Yu, Y. Lu, H. Yu, *Colloids and Surfaces A: Physicochemical and Engineering Aspects* **2023**, *658*, 130672.
[50] H. Yang, Z. Wang, Q. Zhou, C. Xu, J. Hou, *Microchim Acta* **2019**, *186*, 631.
[51] P. Preechakasedkit, N. Nawaukkaratharnant, K. Teekayupak, A. Lomae, N. Ruecha, *Journal of Science: Advanced Materials and Devices* **2023**, *8*, 100535.
[52] N. Janmee, P. Preechakasedkit, N. Rodthongkum, O. Chailapakul, P. Potiyaraj, N. Ruecha, *Anal. Methods* **2021**, *13*, 2796.
[53] N. S. Rashed, S. Zayed, A. Abdelazeem, F. Fouad, *Microchemical Journal* **2020**, *157*, 105069.
[54] R. Zhang, S. He, C. Zhang, W. Chen, *J. Mater. Chem. B* **2015**, *3*, 4146.